Sources and trends of contaminants in a shallow lake in the Mediterranean area from sediment archives of the Anthropocene

Gravina Paola (paolagravi@gmail.com)
Università degli Studi di Perugia: Universita degli Studi di Perugia
Bartolomeo Sebastiani
University of Perugia: Universita degli Studi di Perugia
Federica Bruschi
University of Perugia: Universita degli Studi di Perugia
Chiara Petroselli
University of Perugia: Universita degli Studi di Perugia
Beatrice Moroni
University of Perugia: Universita degli Studi di Perugia
Roberta Selvaggi
University of Perugia: Universita degli Studi di Perugia
Enzo Goretti
University of Perugia: Universita degli Studi di Perugia
Matteo Pallottini
University of Perugia: Universita degli Studi di Perugia
Alessandro Ludovisi
University of Perugia: Universita degli Studi di Perugia
David Cappelletti
University of Perugia: Universita degli Studi di Perugia

Research Article

Keywords: Shallow lake, sediment cores, geochemical baseline, trace elements, Pb isotopes

Posted Date: April 22nd, 2022

DOI: https://doi.org/10.21203/rs.3.rs-1314354/v1

Sources and trends of contaminants in a shallow lake in the Mediterranean area from sediment archives of the Anthropocene

Paola Gravina[1*], Bartolomeo Sebastiani[1], Federica Bruschi[1], Chiara Petroselli[1], Beatrice Moroni[1], Roberta Selvaggi[1], Enzo Goretti[1], Matteo Pallottini[1], Alessandro Ludovisi[1] and David Cappelletti[1]

[1*]Department of Chemistry Biology and Biotechnology, University of Perugia, via Elce di Sotto 8, Perugia, 60123, Umbria, Italy.

*Corresponding author(s). E-mail(s): paolagravi@gmail.com;
Contributing authors: bartolomeo.sebastiani@unipg.it;
federica.bruschi@studenti.unipg.it; petrosellichiara@gmail.com;
b.moroni@tiscali.it; roberta.selvaggi@unipg.it;
enzo.goretti@unipg.it; matteo.pallottini@unipg.it;
alessandro.ludovisi@unipg.it; david.cappelletti@unipg.it;

Abstract

In this study, the anthropogenic contamination in Trasimeno lake (Central Italy) was investigated using three sediment cores of the last 150 years (Anthropocene) to identify the primary sources of pollutions and quantify the level of contaminant enrichment in the basin. To this aim, trace elements, polycyclic aromatic hydrocarbons, and lead isotope ratios have been determined at biannual resolution. The deeper parts of the sediment cores were used to estimate the local geochemical baseline, based on known statistical methods, and to determine the values of enrichment factors. Principal component analysis and factor analysis were exploited to associate chemical proxies to human-driven contamination processes. On these grounds it was possible to identify the timings

and impacts of pre-world war industrial productions and more recent activities characteristic of the basin's surroundings, such as agriculture.

Keywords: Shallow lake, sediment cores, geochemical baseline, trace elements, Pb isotopes

1 Introduction

Freshwater ecosystems such as lakes and rivers are critical to understanding the effects of the environmental change driven by human activities, which have been particularly relevant in the Anthropocene Dubois et al (2018). To assess the impact of human activities, an undisturbed reference, such as pristine natural background sediments, is necessary to reflect the situation of the individual lake on a local or regional scale. A background concentration is defined as the concentration of trace elements before industrialisation, so its level should reflect natural processes uninfluenced by human activities (Tapia et al (2012); Tylmann (2005)). However, this reference is not easy to obtain because of the rapid population growth, industrialization, and urbanization processes over the past two centuries.

In the present work, we focus on Trasimeno, a shallow lake in Central Italy, which, similar to other basins in the Mediterranean area, has been severely impacted by human activities, which have altered its sensitive hydrological status since the beginning of the twenty century and affected the ecosystem and biota (Goretti et al (2016)). Recently, exploiting high-resolution stratigraphic archives (Gravina et al (accepted 2022)), we characterized the three major hydrological regimes of the lake, focussing on the variations of precipitation and sedimentation processes of endogenic carbonates, calcite, and calcium carbonate phosphate and relating the presence of these compounds to natural

and human-driven processes. This study allowed us to identify the range of the sedimentary archives less impacted by anthropogenic processes.

Herein, we started from this piece of knowledge to define a geochemical baseline which allowed us to identify and date the primary sources of pollution affecting the Trasimeno lake and quantify the degree of contaminant enrichment. Three short sediment cores have been exploited to this aim and characterized in terms of major and trace elements, polycyclic aromatic hydrocarbons, and lead isotope ratios. Data have been further processed by multivariate analysis and discussed. The significant human impacts have been classified into three periods covering the Anthropocene and encompass artificial water level manipulation, industrial activities in the pre-second World War period, and more recent eutrophication related to agricultural practices.

2 Materials and Methods

2.1 Study area, sampling and processing

The Trasimeno Lake is a shallow and closed basin located in Central Italy. Despite its large extension (124 km^2), which makes it the largest lake of central and southern Italy, the lake is very shallow, and its bathymetry is very smooth (Figure $SM1 - a$). In the last two centuries, the hydrometric trend of the basin passed through 3 distinct phases: (i) an old phase (OP) (from 1860 to 1900), during which the water level exceeded the overflow level (257,5 m a.s.l.), allowing the discharge of suspended materials to the outside; (ii) a middle phase (MP) (from 1900 to 1960), during which the water level remained below the overflow level and also suffered a substantial lowering, causing saturation of the components in the water column; (iii) a young phase (YP) (from 1960 to 2010), during which the water level rose but not above the overflow level (Figure $SM1 - b$) The present study has characterized three sediment cores

covering the 1860-2010 period and superficial sediments sampled during 2018 (Figure $SM1 - a$ and table in Figure $SM2$). The cores have been cut at biennial resolution, dated, and finally a portion of each section has been acid digestion or extracted in a proper solvent for the subsequent chemical analyses. All the details of the sampling site and sediment cores processing are reported in (Gravina et al (accepted 2022)).

2.2 Chemical analysis

Major and trace elements (Al, Fe, Ti, V, P and Mn, Co, Ni, Pb, Cr, Cu, Zn) concentrations were determined by Inductively Coupled Plasma an Optical Emission Spectrometry (ICP-OES, Ultima 2, HORIBA Scientific) equipped with an ultrasonic nebulizer (CETAC Technologies, U-5000AT). Analytical wavelengths are reported in Table $SM1$. PAHs have been analysed using a gas chromatography-mass spectrometry with a triple-axis detector (HP7890A/5975CVL - Agilent Technologies, USA), equipped with a low bleed Select-PAH capillary column (Agilent J&W, CP 7461). The determination of $^{208}Pb/^{207}Pb$ and $^{206}Pb/^{207}Pb$ ratios was performed by an Agilent 8900 ICP-MS/MS (100 version, Agilent Technologies, Japan), operated in the MS/MS mode. The collision reaction cell was pressurized with a NH_3/He 15 % mixture, used as a damping gas to lower the RSD. The instrumental mass bias was corrected with the standard sample bracketing method using the lead isotopic standard SRM 981 from NIST (Gaithersburg, MD, USA) (Vanhaecke et al (2009); Bazzano and Grotti (2014); Bazzano et al (2021); Bertinetti et al (2022)). The Supplementary Material (Section 1 - Chemical analysis) reports more details on the analytical methodologies.

A standard principal component analysis (PCA) and a factor analysis (FA) have been performed on the chemical dataset with R - Version 1.2.5033 using the packages *tidyverse* and *factoextra*.

2.3 Geochemical baseline and enrichment factors

In this study, the geochemical baseline (GBL) was obtained using the bottom portions of the 3 sediment cores (approximately 25 cm), considering that these portions represent the least contaminated sediments due to their deposition before 1900. Then, two different GBLs were calculated using passive methods, the relative cumulative frequency technique (RCF) and the linear regression method (LRM).

The RCF technique is commonly used to obtain GBL (Matschullat et al (2000); Teng et al (2009)) of an individual element and is based on different slopes of the relative cumulative frequency content fitting curves for the natural origin and abnormal concentration. A bend of the slope in the upper part of the curve (higher values) can be used to distinguish between anthropogenically non-influenced samples (low values) and anthropogenically influenced samples (high values). The baseline is obtained from the data below the first inflection value. The data in the cumulative frequency curve are tested with a linear regression method, until achievement of the condition of $p < 0{,}05$ and $R^2 > 0{,}9$. Otherwise the maximum value is removed and the procedure is repeated until the two criteria are both met.

The LRM allows obtaining the regional GBL from deep sediments by plotting the element towards the normalizer (Selvaggi et al (2020)) According to the principle of normalization, the relative proportions of metals within materials from a particular region tend to be constant, even if the absolute metal concentration varies between crustal elements from one region to another. In

the present study, normalization was done with Al or Fe according to the best correlation with the element considered. The samples lying beyond the confidence interval of 95% have been labeled as anthropogenically influenced. In the linear relationship between each element of concern and the reference elements (e.g. Al or Fe), data lying out of the 95% confidence band are eliminated, a new linear equation is built with the updated data set and, the process goes on until all the data are within the 95% confident band.

The local GBL was used in the present study to improve the assessment of anthropogenic impact through the enrichment factor (EF). The EFs are calculated as:

$$EF = \frac{\left(\frac{[Me]}{[X]}\right)_{sample}}{\left(\frac{[Me]}{[X]}\right)_{reference}}$$

where [Me] is the concentration of the element, [X] is the concentration of the reference element (Al, Fe, V, Li or Sc); at the numerator, there is the sample, while at the denominator there is the reference baseline (Schropp et al (1990)). Al was chosen as the reference for the present study.

3 Results and Discussions

3.0.1 Geochemical Baseline

Two different methods were screened to identify the better GBL as representative of the maximum pristine state of the sampled Trasimeno sediments, in order to quantify the enrichment of the trace elements through the EF factors.

An example of the RCF values provided by cumulative frequency curves method are plotted in the Figure 1 for the cases of Co and Cr (other elements are in Supplementary Material in Figure SM4). Figure 2, instead, shows the linear regression method for calculating GBL, where Al or Fe are chosen

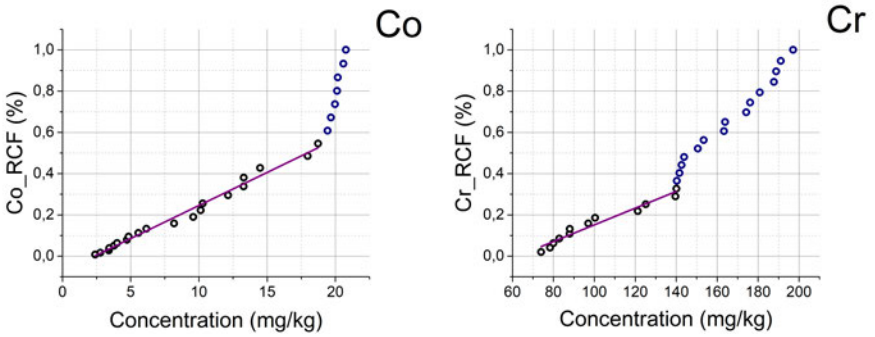

Fig. 1 Cumulative frequency curves (scatters) of Co and Cr. Co represents the curve with only 1 inflection point, while Cr represents the curve with 2 inflection points. Linear regressions were performed on the cumulative frequency curve with $p<0.01$ and $R2>0.9$ (purple line).

according to the highest correlation value with the element considered. Both GBLs obtained through RCF and linear regression methods are shown in the Table 1. Eventually, Background (Bkg) values, also reported in the Table 1, were calculated by arithmetic average of the bottom part of the cores (portion before 1900s corresponding to the pre-industrial period).

As shown in Table 1, the RCF is the closest lacustrine sediment baseline to other baseline values from different areas of the world (e.g. Callender (2014)). As regards Ni, Cd and Cr the RCF baselines are higher than those reported by Callender (2014). While the RCF baselines for Pb, Cu and Zn are lower than Callender (2014) values, being 11, 16 and 70 ppm compared to 22, 34 and 97 ppm, respectively.

3.0.2 Enrichment factors and trends of contaminants

EF values were calculated using the RCF baseline, considering that, even if widely used as a sediment metal-enrichment assessment tool, the calculated EF is highly dependent on the choice of an appropriate background or baseline as reference level (Rubio et al (2000)). Interpretation of EF values allows the assessment of contaminant enrichment. According to Birch et al (1996),

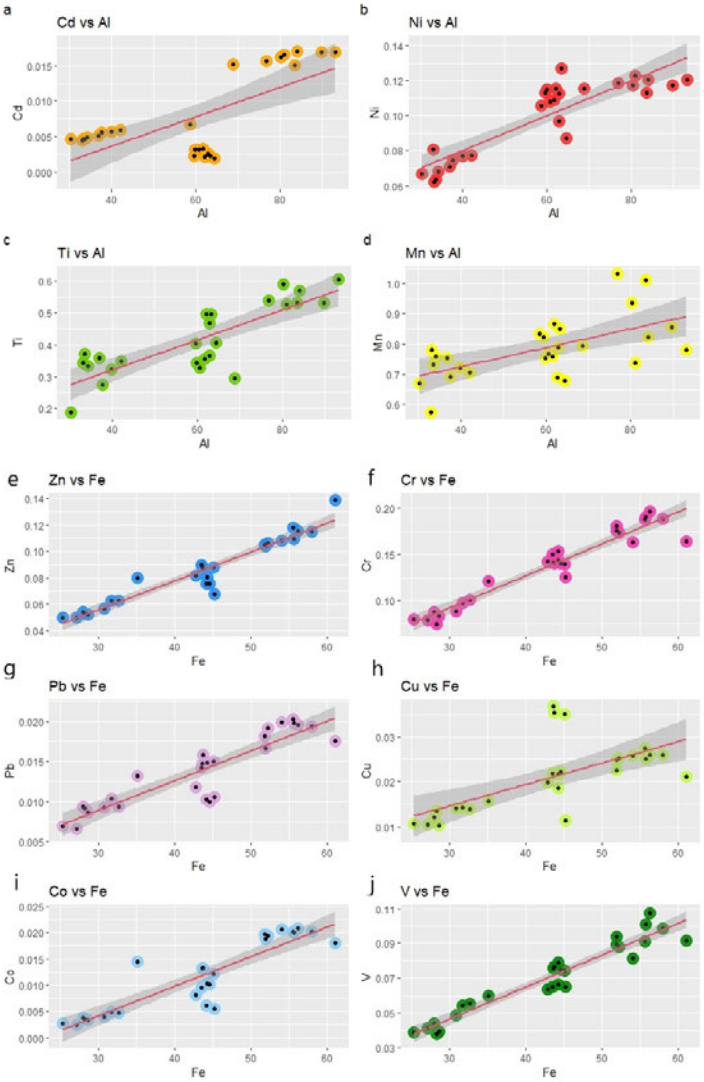

Fig. 2 Normalisation of heavy metals on the reference element: Al (from *a* to *d*) and Fe (from *e* to *j*) of bottom dataset. Concentration are in mg/kg. The linear regression was obtain with $p < 0.01$ and R^2 greater. The dark grey area represents the 95% confidence.

there were several scenarios : EF $<$ 1 "no enrichment", 1 $<$ EF $<$ 3 "minor enrichment", 3 $<$ EF $<$ 5 "moderately enrichment", 5 $<$ EF $<$ 10 " moderately enrichment", 10 $<$ EF $<$ 25 "severe enrichment" 25 $<$ EF $<$ 50 "very

severe enrichment" and EF $>$ 50 "extremely severe enrichment". The EFs values were also interpreted by Zhang and Liu (2002): when EF is between 0.5 and 1, the metal could be mainly from the weathering process; while if EF is greater than 1.5, the metal is from anthropogenic sources or grater percentage of the metal is from no-natural process.

The boxplot, reported in Figure SM5 in Supplementary Material, shows means, high and low quartiles and outliers for the EF values in the 3 sediment cores (C1,C2,C3).

The enriched elements in C2 (Figure 3), listed in descending order, are Co, Pb, Zn, Mn, P, Cu, Ti, Cr, V, and Ni. The enriched elements, listed in descending order for C1 core are Cu, Pb, Co, Ni, Zn, Cr, V, Mn, P, and Ti; while for C3 core are Pb, Zn, Cu, Ni, Cr, V, Mn, Co, Ti, and P. The global anthropogenic enrichment in the basin seems to be high, especially for Pb, Cu, Co, and Zn.

3.0.3 Trends of polycyclic aromatic hydrocarbons

Specific organic proxies such as some polycyclic aromatic hydrocarbons (PAHs) allow to identify their possible source, which can be petrogenic, pyrogenic, biogenic, and diagenetic (Abdel-Shafy and Mansour (2016)). The pyrogenic kind of PAHs is linked to exposure to high temperatures under low oxygen or no-oxygen conditions, such as wood and coal combustion. The petrogenic origin is due to transportation, storage, and spills of crude oil and crude oil products. In contrast, the biological origin of some PAHs is due to their synthesis by certain plants and bacteria or to their formation during degradation of vegetative matter. For the estimation of anthropogenic sources, Perylene is usually removed from the sum of PAHs, because it is formed after deposition transformation during diagenesis and is derived from natural precursors (Jiang et al

Methods	GBL / Bkg		Co	Ni	P	Pb	Cr	Cu	Ti	Zn	Mn	V
Relative cumulative	Core sed	**Mean**	8.46	72.82	1381,04	10.59	101.23	16.14	325.09	69.69	758.04	64.10
frequency methods (RCF)		dev sta	5.14	7.99	157,59	2.53	24.09	4.62	49.73	14.70	69.26	17.23
Linear regression	Core sed	**Mean**		85.83	1798,06				447.61		823.45	
techinque - Al		dev staa		23.87	387,72				143.59		124.12	
Linear regression	Core sed	**Mean**	13.00			14.91	134.89	19.19		86.20		66.13
techinque - Fe		dev sta	7.50			4.75	43.59	5.95		23.85		23.15
Baseline mean	Core sed	**Mean**	11.48	99.11	1680,05	13.73	137.42	20.82	415.41	84.19	784.26	70.48
3 bottom cores		dev sta	6.81	21.79	441,74	4.44	39.39	7.74	111.02	24.77	100.77	20.79
Bottom core C1	Core sed	**Mean**	10.66	108.98	1497,81	13.48	144.11	24.41	406.82	87.17	780.99	73.207
		dev sta	3.70	10.86	77,26	2.63	10.20	8.43	65.242	19.36	64.43	8.595
Bottom core C2	Core sed	**Mean**	19.93	118.13	2272,85	19.09	182.41	25.36	523.20	110.03	871.76	93.86
		dev sta	0.65	3.14	97,92	1.16	10.92	1.37	97.07	5.37	110.25	8.32
Bottom core C3	Core sed	**Mean**	4.87	71.23	1292,26	9.23	89.98	12.79	317.27	57.91	710.12	46.68
		dev sta	3.69	6.58	190,90	1.90	14.51	2.00	59.95	9.54	61.97	8.21
Current state	Core sed	**Mean**	10,7	76,6	418,6	18,8	100,0	18,2	292,5	78,5	1063,9	53,3
		dev sta	3,7	16,2	79,1	3,0	27,6	4,1	104,4	13,1	303,9	17,6
Förstner and Wittmann (1981)	Lake sed	**Mean**		44.5		27	42	30		65.5		
Pre-indsutrial	Lake sed	**Mean**		40		22	48	34		97		
Callender (2014)												
Recent lacustrine	Lake sed	**Mean**		39		102	63	60		207		
Callender (2014)												

Table 1 Concentration of geochemical baseline and background values calculated with different methods. All data are presented as mg/Kg or ppm.

198 (2000)). Therefore, the total PAH (=ΣPAHs) is calculated by subtracting the
199 perylene concentration in the following.

200 As shown in Fig. 4 - *a*), ΣPAHs) was relatively constant until 1920 with an
201 average value of 26.5 ng/g. This value is consistent with those found in surface
202 sediments of relatively pristine environments in the Italian alps (Poma et al
203 (2017)). In the MP hydrological phase we observed a significant increase of
204 ΣPAHs, starting in 1930-40, and reaching values a factor 4 higher in the YP,
205 after WW II with a first maximum in 1965-70 and a second maximum in the
206 late 1990s (Figure 4 - *a*). On the other side, Perylene remained constant and low
207 during the most recent YP phase but increased rapidly with the depth of burial
208 in sediments due to diagenesis, unlike other PAHs molecules (Figure 4 - *b*). We
209 exploited specific diagnostic ratios (typically based on isomers) to identify the
210 contamination sources (Roszko et al (2020); Yunker et al (2002)), assuming
211 that different PAH molecules transform and degrade at the same rate during
212 their lifetime in the environment, so that the characteristic concentration ratios
213 of the sources are preserved. A scatterplot of the two PAHs diagnostic ratios
214 obtained for the Trasimeno core sediments, is shown in Figure 4 - *c*. The
215 Flu/(Flu + Pyr) ratio distinguishes the origin of samples belonging to different
216 historical moments (Guo et al (2011)). The Trasimeno sediment samples from
217 the period of most significant industrial activity, i.e. around the Second World
218 War, indicate oil and liquid fossil fuel combustion sources. Most YP samples
219 represented anthropogenic origin related to biomass combustion and generated
220 by pyrolysis, which can be associated with characteristic agricultural activities
221 of the surroundings of Trasimeno lake in the last part of the 20^{th} century.

3.1 Identification of anthropogenic sources by PCA and FA analysis

A PCA analysis was performed on the C2 central core, which has the largest number of samples and which is more undisturbed and representative of the entire basin. The PCA performed on the C2 included trace elements and ΣPAHs (Figure 5 and Table SM4). The analysis identified 5 groups of tracers: one natural group (A) including Al, Ti, V and Fe and 4 distinct anthropogenic groups (B, C; D and Pb). Group *B* included Co, Ni, Zn and Cr, group *C* included Cu and P, and *D* included Mn and ΣPAHs. In addition, the Mn variable is explained in part also by PC1. Pb is an isolated element that is separated from the groups mentioned above and is explained mainly by PC2.

The score legend of Figure 5 effectively separates the three different hydrometric phases that have occurred in the lake over the past 150 years (OP, MP and YP), and allows to determine the sources of elements and organic compounds. In particular, the YP scores and PC2 distinguished the anthropogenic element groups (B, C and D groups). The distinct groups of anthropogenic elements have different origins; in fact, the anthropogenic group *B* is well separated from the natural elements (groups *A*) by PC2, but is also well isolated from Pb, which is likely associated with atmospheric deposition due to human use of leaded gasoline since the 1960s.

Finally, the results of the PCA analysis individuated a specific type of contamination throughout the lake, influenced by the intensification of agriculture during the eutrophic phase (YP, after 1970). The use of fertilizers, which can contain Mn, Cu, P, Zn, and Cr, Pb, is the main impacting factor. Manganese can be emitted as Mn sulfates in fertilisers or from pesticides, animal feed, or water treatment products. On the other hand, copper is contained in pesticides and fungicides (used to control plant diseases) or is emitted as Cu sulfate

(treatment used to control algal growth). Actually, Cu sulfate is also added to pig feed to suppress bacterial action and therefore it is poured in the soil when pig slurry is used as fertilizer (Panagos et al (2018)). The use of fungicides based on the mixture of Cu sulfate, lime and water started in 1880s and became widely used to control downy mildew in grapevines, while on the global scale, the use of Cu in agriculture has increased since 1980 (Panagos et al (2018)). Ultimately, the use of both Cu and P as fertilizers has been a common procedure for much of the last century (confirming their appearance in group C), in contrast, the use of Mn as a fertilizer was not approved in Europe until the early 2000s, and that's why Mn does not belong to group C (EFSA Panel (NDA) (2013); (FEEDAP); Christensen (2015)). The increasing trend in PAHs concentrations also correlates with Mn, given the increase of both especially in recent times (confirming the affiliation of PAHs to the group D).

Factor analysis (in supplementary material Figure SM7) confirms the source-dependent separation of elements obtained by the PCA. It is observed that Al and Fe are separated from other elements, representing the group of natural origin, while among the elements of anthropogenic origin, there is the subgroup P-Mn.

3.2 Industrial contamination in the middle hydrological phase

The average concentration of the trace elements (V, Co, Ni, P, Pb, Cr, Cu, Ti, Mn and Zn) measured for the three sediment cores (top part, bottom part - used for GBL calculation - and whole core) together with maximum and minimum values are reported in supplementary material in Table SM3. The trends are qualitatively similar for the three cores (Figure SM3). Nevertheless the highest concentrations have been recorded in C2 (central lake) and the

lowest in C3 (Southern lake). These differences can be associated with the different sedimentation rates (Gaino et al (2012)), the distance from the shore or the centre of the basin, and the different composition of washed-out material from the Eastern, Western, and Southwestern parts (Figure SM1) of the area surrounding the lake Yang and Rose (2005). Observing data reported in Table SM3 for the central C2 core Ni, Cr and Ti have higher concentrations in the bottom with respect to the top of the core, and the current (2018) concentration values drop even further. On the other side V, Co, Cu, Zn have comparable values along with the sediment core, but also show lower values in the most superficial and current sample; unlike previous trends, Pb and Mn present lower mean concentrations in the bottom part of the core with respect to the top part and also with respect to the current (2018) conditions. The situation is slightly different for the north-eastern C1 core: Cu, Pb, Co, Mn and Zn show lower mean concentration values in the bottom part than in the top part and whole core while V presents stable values for the whole core record. In the case of the southern C3 core, V, Co, Ni, Pb, Cr, Cu and Zn present lower mean concentration values in the bottom part of the core than in both the top and the whole sediment core; Ti and Mn present relatively stable values for the entire core record.

A closer view of the concentration profiles of some specific trace elements (Pb, Ni, Co, Zn, Cr, and V) of the C2 core is shown in Figure 6. The concentration trends are characterised by a clear peak dated between 1930-1945 for all the elements. The peak corresponded to a simultaneous increase of the element concentrations and coincided with a relative rise in the water level (see Figure SM1 - *b*), even if in the general context of the lowering phase. Overall, these pieces of evidence point to a significant contamination process lasting more or less 20 years. The nature of the trace elements involved suggests an industrial

source. Indeed, in this period, a military air-plane industry was operative and very active in Passignano, the main village on the lake's northern coast. This air-plane industry moved from Milan to the surroundings of the Trasimeno's shores in 1916, and one of the most important Italian aeronautical schools was also established close to the basin. Technological development began in 1922 when the "$Societa' Aeronautica Italiana$"($SAI$) was created and the combat aircraft production increased significantly with the outbreak of World War II (Bellaveglia (2015) ; SAI (2018)).

After the peak, most elements lowered in concentration while, in the case of Pb, we notice a growth from the 1960s to the present day. This trend must be associated with a different source and reasonably connected with the use of leaded gasoline, containing Pb as an anti-knockout substance (Resongles et al (2021)). A further investigation for the Pb case has been made by measuring the $^{208}Pb/^{207}Pb$ and $^{206}Pb/^{207}Pb$ isotope ratios which are proxies of the emission source. Results are shown in Figure 7 for the $^{206}Pb/^{207}Pb$ together with the trend of the total Pb concentration. A $^{208}Pb/^{207}Pb$ versus $^{206}Pb/^{207}Pb$ plot is presented in the Supplementary Material (Figure SM8). The results in Figure 7 show a clear lowering of the $^{206}Pb/^{207}Pb$ isotope ratio from values larger than 1,230 (1,233 the maximum) previous of 1920, which can be considered a natural situation, towards values less than 1,210 (1,207 the minimum) in the most recent years. Isotope ratio values can vary easily between different areas depending on the mineralogy of the area and on the level and type of contamination from the surrounding. In general, the values obtained in the Trasimeno Lake are consistent with the literature (Odigie et al (2014); Gobeil et al (1995); Townsend and Seen (2012); Chiaradia et al (1997); Brännvall et al (2001)). The lowering of the $^{206}Pb/^{207}Pb$ ratio plotted in Figure 7 started clearly in coincidence with the pollution peak of the 1930-1940 and

carried on further with a minimum in the 1980s and a slight recover later on. According to the literature this particular ratio is higher in natural soils, while it decreased because of anthropogenic pollution (Renberg et al (2002);Sakata et al (2018); Chiaradia et al (1997); Bränvall et al (2001)). Moreover, a three-isotope plot can often help identify and differentiate between anthropogenic and natural/geogenic Pb sources, particularly when the naturally occurring and anthropogenically introduced Pb has significantly different isotope ratios (Townsend and Seen (2012)). We reported in the supplementary material (Figure SM8) the correlation between the $^{208}Pb/^{207}Pb$ and the $^{206}Pb/^{207}Pb$ isotope ratios which, consistently, suggest the contribution of at least two end-members to the observed Pb isotope ratio. In conclusion, the isotope ratio results confirm the anthropogenic nature of the contamination in the 1930-1940 event and the successive anthropogenic origin of Pb in the more recent years.

3.3 Impacts of vehicular traffic and agricultural contaminations in the young hydrological phase

Pb shows a characteristic enrichment trend, which is in good agreement between the different sampling sites. In particular, the trend shows an increase in concentration during the WWII period that persisted until the early 2000s. As discussed above, Pb enrichment is primarily due to anthropogenic activities such as the use of leaded gasoline and the disposal of sewage sludge to the ground: only core C1 showed a lowering of enrichment after 2000, indicating the termination of leaded gasoline use, which came into effect in 2002 in Europe. The C1 core is located in the area of the lake most impacted by vehicular traffic due to the presence of a highway, built in the 1965, at 200m from the shore.

The intensification of the agricultural activities in the YP is responsible for the release of various elements and pollutants in the environment, such as the essential elements (Cu and Zn) contained in fertilisers, and the heavy metals (Pb and Cr) used in the synthesis of fertilisers as catalysts (Nacke et al (2013). Moreover, the use of leaded fuel in agricultural machinery for the development of farming operations is another reason for enrichment of Pb (Nicholson et al (2003); Zan et al (2012)).

Cu is consistently enriched in the sampled sediments, with maximum values recorded between 1970 and 1980. One of the main sources of Cu in the Trasimeno basin is the use of Cu sulphate pentahydrate in the production of fungicides, introduced in agriculture as early as the $19th$ century and widely distributed on fruit plants (olives and vines) and vegetables. Other sources of land pollution are sewage sludge, municipal compost and animal waste (Callender (2014)). Mn enrichment began only later in 1965, with a maximum enrichment around the 1990s, confirming the delay in using this element for agricultural purposes towards the end of the century.

The current state of the sediment showed that pollution caused by some elements and heavy metals, such as Cu, Co, Ni , Cr, Zn, P and V has returned to baseline levels after increasing during the industrialization, urbanization and agricultural intensification. On the other hand, elements like Pb, Mn, Cu and Zn maintain enriched values relative to the baseline but lower than the period between 1940-1990. Mn and Cu are currently used in the predominant agricultural activities around the Trasimeno lake. The Pb enrichment may be due to the persistence of lead contamination even after the cessation of leaded petrol use in the early 2000s (Resongles et al (2021)). The process of remobilization of historical Pb deposited in soil from the atmosphere can be considered a critical current secondary source (MacKinnon et al (2011)).

4 Conclusion

A set of short sediment cores have been used to identify he natural baseline and quantify the anthropogenic contamination in the context of a fragile shallow lake in Central Italy. The challenge was to disentangle the pollution effects from the human alteration of the hydrological regime of the lake, which during 150 years produced three distinct hydrometric phases. The main proxies identified to investigate the lake pollution have been industrial metals (Cr and Zn), elements used in agriculture (Cu, Mn and P) and some specific organic compounds of anthropogenic and natural origin (PAHs). Pb isotope ratios have also been exploited to attribute the nature of the intense industrial event. In addition, the determination of the local baseline by using deep sediment cores by the RCF statistical method ensured the quantification of sediment enrichment by pollutants. The impact of industrial pollution at the regional level starting before the 2nd World War mainly tied up to the increase in the airplane industry activities in Passignano. Over time, the main causes responsible for the input of pollutants into the lake become intensification of agriculture, livestock, urban and transportation, which have increased since the 1960s. The assumption made to obtain the local baseline seemed adequate, according to the comparison with global baseline values in the literature and the variability of the enrichments describing the human activities around Trasimeno. The assessment of the current condition of the lake demonstrated that some elements such as Cu, Co, Ni , Cr and V, mainly related with industrialization, urbanization and agriculture has returned to GBL levels. On. the other side, Mn and Pb, used in intensive agricultural activities and highly persistent in the environment even after being banned at the end of the last century, respectively, remain enriched compared to GBL values.

Acknowledgments. We thank MIUR and University of Perugia for financial support through AMIS project ("Dipartimenti di Eccellenza–2018–2022").

References

Abdel-Shafy HI, Mansour MS (2016) A review on polycyclic aromatic hydrocarbons: Source, environmental impact, effect on human health and remediation. Egyptian Journal of Petroleum 25(1):107–123. doi:https://doi.org/10.1016/j.ejpe.2015.03.011

Bazzano A, Grotti M (2014) Determination of lead isotope ratios in environmental matrices by quadrupole ICP-MS working at low sample consumption rates. Journal of Analytical Atomic Spectrometry 29(5):926. doi:https://doi.org/10.1039/c3ja50388g

Bazzano A, Bertinetti S, Ardini F, et al (2021) Potential Source Areas for Atmospheric Lead Reaching Ny-Ålesund from 2010 to 2018. Atmosphere 12(3):388. doi:https://doi.org/10.3390/atmos12030388

Bellaveglia C (2015) Aeronautica Sul Trasimeno: Storia Della "SAI Ambrosini" Di Passignano. Murena editrice, Perugia

Bertinetti S, Bolea-Fernandez E, Malandrino M, et al (2022) Strontium isotopic analysis of environmental microsamples by inductively coupled plasma – tandem mass spectrometry. Journal of Analytical Atomic Spectrometry 37(1):103–113. doi:https://doi.org/10.1039/D1JA00329A

Birch L, Hanselmann KW, Bachofen R (1996) Heavy metal conservation in Lake Cadagno sediments: Historical records of anthropogenic emissions in a meromictic alpine lake. Water Research 30(3):679–687. doi:https://doi.org/10.1016/0043-1354(95)00231-6

Bränvall ML, Bindler R, Emteryd O, et al (2001) [No title found]. Journal of Paleolimnology 25(4):421–435. doi:https://doi.org/10.1023/A:1011186100081

Callender E (2014) Heavy Metals in the Environment – Historical Trends. In: Treatise on Geochemistry. Elsevier, p 59–89, doi:https://doi.org/10.1016/

437 B978-0-08-095975-7.00903-7

438 Chiaradia M, Chenhall B, Depers A, et al (1997) Identification of historical
439 lead sources in roof dusts and recent lake sediments from an industrialized
440 area: Indications from lead isotopes. Science of The Total Environment
441 205(2-3):107–128. doi:https://doi.org/10.1016/S0048-9697(97)00199-X

442 Christensen F (2015) Survey of manganese(II) sulphate: part of the LOUS
443 review. Danish Environmental Protection Agency

444 Dubois N, Saulnier-Talbot É, Mills K, et al (2018) First human impacts and
445 responses of aquatic systems: A review of palaeolimnological records from
446 around the world. The Anthropocene Review 5(1):28–68. doi:https://doi.
447 org/10.1177/2053019617740365

448 EFSA Panel (NDA) (2013) Scientific Opinion on Dietary Reference Values
449 for manganese. EFSA Journal 11(11). doi:https://doi.org/10.2903/j.efsa.
450 2013.3419

451 (FEEDAP) E (2016) Safety and efficacy of manganese compounds (E5) as feed
452 additives for all animal species: Manganous carbonate; manganous chlo-
453 ride, tetrahydrate; manganous oxide; manganous sulphate, monohydrate;
454 manganese chelate of amino acids, hydrate; manganese chelate of glycine,
455 hydrate, based on a dossier submitted by FEFANA asbl. EFSA Journal
456 14(2). doi:https://doi.org/10.2903/j.efsa.2016.4395

457 Förstner U, Wittmann GTW (1981) Metal Pollution in the Aquatic Environ-
458 ment. Springer Berlin Heidelberg, Berlin, Heidelberg

459 Gaino E, Scoccia F, Piersanti S, et al (2012) Spicule records of Ephydatia
460 fluviatilis as a proxy for hydrological and environmental changes in the
461 shallow Lake Trasimeno (Umbria, Italy). Hydrobiologia 679(1):139–153.
462 doi:https://doi.org/10.1007/s10750-011-0861-7

Gobeil C, Johnson WK, Macdonald RW, et al (1995) Sources and Burden of Lead in St. Lawrence Estuary Sediments: Isotopic Evidence. Environmental Science & Technology 29(1):193–201. doi:https://doi.org/10.1021/es00001a025

Goretti E, Pallottini M, Ricciarini M, et al (2016) Heavy metals bioaccumulation in selected tissues of red swamp crayfish: An easy tool for monitoring environmental contamination levels. Science of The Total Environment 559:339–346. doi:https://doi.org/10.1016/j.scitotenv.2016.03.169

Gravina P, Ludovisi A, Moroni B, et al (accepted 2022) Geochemical proxies and mineralogical fingerprints of sedimentary processes in a closed shallow lake basin since 1850. Aquatic Geochemistry

Guo JY, Wu FC, Zhang L, et al (2011) Screening Level of PAHs in Sediment Core from Lake Hongfeng, Southwest China. Archives of Environmental Contamination and Toxicology 60(4):590–596. doi:https://doi.org/10.1007/s00244-010-9568-4

Jiang C, Alexander R, Kagi RI, et al (2000) Origin of perylene in ancient sediments and its geological significance. Organic Geochemistry 31(12):1545–1559. doi:https://doi.org/10.1016/S0146-6380(00)00074-7

MacKinnon G, MacKenzie A, Cook G, et al (2011) Spatial and temporal variations in Pb concentrations and isotopic composition in road dust, farmland soil and vegetation in proximity to roads since cessation of use of leaded petrol in the UK. Science of The Total Environment 409(23):5010–5019. doi:https://doi.org/10.1016/j.scitotenv.2011.08.010

Matschullat J, Ottenstein R, Reimann C (2000) Geochemical background - can we calculate it? Environmental Geology 39(9):990–1000. doi:https://doi.org/10.1007/s002549900084

Nacke H, Gonçalves AC, Schwantes D, et al (2013) Availability of Heavy Metals (Cd, Pb, and Cr) in Agriculture from Commercial Fertilizers. Archives of Environmental Contamination and Toxicology 64(4):537–544. doi:https://doi.org/10.1007/s00244-012-9867-z

Nicholson F, Smith S, Alloway B, et al (2003) An inventory of heavy metals inputs to agricultural soils in England and Wales. Science of The Total Environment 311(1-3):205–219. doi:https://doi.org/10.1016/S0048-9697(03)00139-6

Odigie KO, Cohen AS, Swarzenski PW, et al (2014) Using lead isotopes and trace element records from two contrasting Lake Tanganyika sediment cores to assess watershed – Lake exchange. Applied Geochemistry 51:184–190. doi:https://doi.org/10.1016/j.apgeochem.2014.10.007

Panagos P, Ballabio C, Lugato E, et al (2018) Potential Sources of Anthropogenic Copper Inputs to European Agricultural Soils. Sustainability 10(7):2380. doi:https://doi.org/10.3390/su10072380

Poma G, Salerno F, Roscioli C, et al (2017) Persistent organic pollutants in sediments of high-altitude alpine ponds within stelvio national park, italian alps. Inland Waters 7(1):34–44. doi:https://doi.org/10.1080/20442041.2017.1294345, URL https://doi.org/10.1080/20442041.2017.1294345, https://arxiv.org/abs/https://doi.org/10.1080/20442041.2017.1294345

Renberg I, Brännvall ML, Bindler R, et al (2002) Stable lead isotopes and lake sediments—a useful combination for the study of atmospheric lead pollution history. Science of The Total Environment 292(1-2):45–54. doi:https://doi.org/10.1016/S0048-9697(02)00032-3

Resongles E, Dietze V, Green DC, et al (2021) Strong evidence for the continued contribution of lead deposited during the 20th century to the

atmospheric environment in London of today. Proceedings of the National Academy of Sciences 118(26):e2102791,118. doi:https://doi.org/10.1073/pnas.2102791118

Roszko MŁ, Juszczyk K, Szczepańska M, et al (2020) Background levels of polycyclic aromatic hydrocarbons and legacy organochlorine pesticides in wheat sampled in 2017 and 2018 in Poland. Environmental Monitoring and Assessment 192(2):142. doi:https://doi.org/10.1007/s10661-020-8097-5

Rubio B, Nombela M, Vilas F (2000) Geochemistry of Major and Trace Elements in Sediments of the Ria de Vigo (NW Spain): An Assessment of Metal Pollution. Marine Pollution Bulletin 40(11):968–980. doi:https://doi.org/10.1016/S0025-326X(00)00039-4

SAI (2018) SAI Società Aeronautica Italiana

Sakata M, Xu H, Mashio AS (2018) Analysis of historical trend of pollution sources of lead in Tokyo Bay based on lead isotope ratios in sediment core. Journal of Oceanography 74(2):187–196. doi:https://doi.org/10.1007/s10872-017-0448-7

Schropp SJ, Lewis FG, Windom HL, et al (1990) Interpretation of Metal Concentrations in Estuarine Sediments of Florida Using Aluminum as a Reference Element. Estuaries 13(3):227. doi:https://doi.org/10.2307/1351913

Selvaggi R, Damianić B, Goretti E, et al (2020) Evaluation of geochemical baselines and metal enrichment factor values through high ecological quality reference points: A novel methodological approach. Environmental Science and Pollution Research 27(1):930–940. doi:https://doi.org/10.1007/s11356-019-07036-3

Tapia J, Audry S, Townley B, et al (2012) Geochemical background, baseline and origin of contaminants from sediments in the mining-impacted Altiplano and Eastern Cordillera of Oruro, Bolivia. Geochemistry: Exploration, Environment, Analysis 12(1):3–20. doi:https://doi.org/10.1144/1467-7873/10-RA-049

Teng Y, Ni S, Wang J, et al (2009) Geochemical baseline of trace elements in the sediment in Dexing area, South China. Environmental Geology 57(7):1649–1660. doi:https://doi.org/10.1007/s00254-008-1446-2

Townsend AT, Seen AJ (2012) Historical lead isotope record of a sediment core from the Derwent River (Tasmania, Australia): A multiple source environment. Science of The Total Environment 424:153–161. doi:https://doi.org/10.1016/j.scitotenv.2012.02.011

Tylmann W (2005) Lithological and geochemical record of anthropogenic changes in recent sediments of a small and shallow lake (Lake Pusty Staw, northern Poland). Journal of Paleolimnology 33(3):313–325. doi:https://doi.org/10.1007/s10933-004-5506-7

Vanhaecke F, Balcaen L, Malinovsky D (2009) Use of single-collector and multi-collector ICP-mass spectrometry for isotopic analysis. Journal of Analytical Atomic Spectrometry 24(7):863. doi:https://doi.org/10.1039/b903887f

Yang H, Rose N (2005) Trace element pollution records in some UK lake sediments, their history, influence factors and regional differences. Environment International 31(1):63–75. doi:https://doi.org/10.1016/j.envint.2004.06.010

Yunker MB, Macdonald RW, Vingarzan R, et al (2002) PAHs in the Fraser River basin: A critical appraisal of PAH ratios as indicators of PAH source and composition. Organic Geochemistry 33(4):489–515. doi:https://doi.

org/10.1016/S0146-6380(02)00002-5

Zan F, Huo S, Xi B, et al (2012) A 100-year sedimentary record of natural and anthropogenic impacts on a shallow eutrophic lake, Lake Chaohu, China. Journal of Environmental Monitoring 14(3):804. doi:https://doi.org/10.1039/c1em10760g

Zhang J, Liu C (2002) Riverine Composition and Estuarine Geochemistry of Particulate Metals in China—Weathering Features, Anthropogenic Impact and Chemical Fluxes. Estuarine, Coastal and Shelf Science 54(6):1051–1070. doi:https://doi.org/10.1006/ecss.2001.0879

Declarations

- Funding -This work was supported by MIUR and University of Perugia for financial support through AMIS project ("Dipartimenti di Eccellenza–2018–2022").
- Conflict of interest/Competing interests - The authors declare that they have no known competing financial interests or personal relationships that could have appeared to influence the work reported in this paper.
- Ethics approval - Not applicable
- Consent to participate -Yes
- Consent for publication - Yes
- Availability of data and materials -Yes
- Authors' contributions - All authors contributed to the study. Material preparation, data collection and analysis were performed by [Paola Gravina], [Federica Bruschi], [David Cappelletti]. The first draft of the manuscript was written by [Paola Gravina] and all authors [Bartolomeo Sebastiani], [Federica Bruschi], [Chiara Petroselli], [Beatrice Moroni], [Roberta Selvaggi], [Enzo Goretti], [Matteo Pallottini], [Alessandro Ludovisi], [David

Cappelletti] commented on previous versions of the manuscript. All authors [Bartolomeo Sebastiani], [Federica Bruschi], [Chiara Petroselli], [Beatrice Moroni], [Roberta Selvaggi], [Enzo Goretti], [Matteo Pallottini], [Alessandro Ludovisi], [David Cappelletti] read and approved the final manuscript.

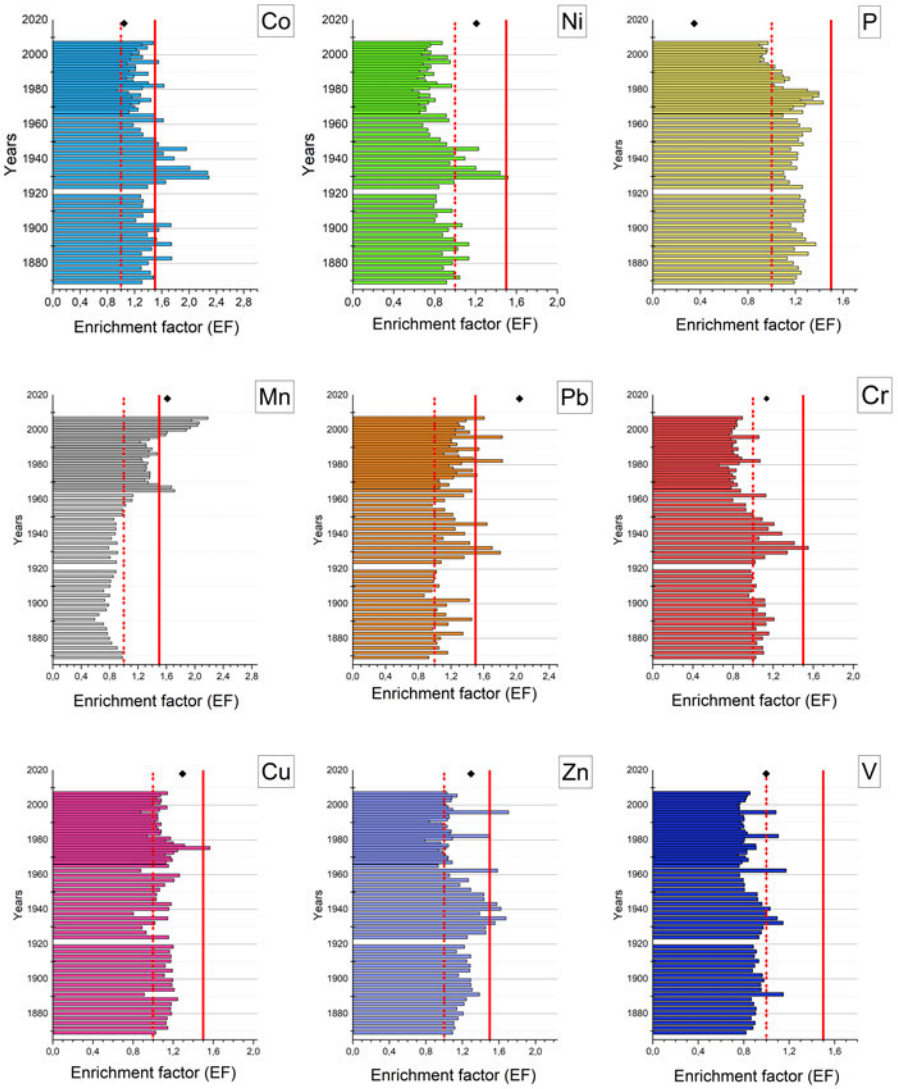

Fig. 3 C2 core trend of enrichment factors for trace elements (Co, Ni, P, Mn, Pb, Cr, Cu, Zn and V) represented by the histogram graph. The black rumble represents the current state of enrichment in the surface sediments of the lake (corresponding to 2018). The dotted red line indicates limit at 1 (according to Birch et al (1996)), while continuous red line indicates limit at 1.5 (according to Zhang and Liu (2002)).

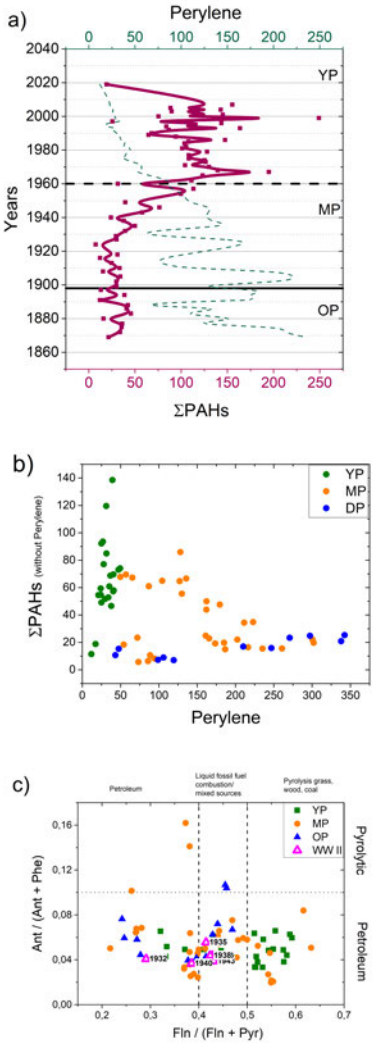

Fig. 4 *a*) ΣPAHs (continuous red curve) and perylene (dashed green line) concentration (ng/g) in core C2; *b*) ΣPAHs versus perylene concentration (diagenetic origin); *c*) scatterplot of Flu/(Flu + Pyr) and Ant/(Ant + Phe) diagnostic ratios with marked regions corresponding to different sources. Square represent samples in YP, circles represent sample in MP, triangles represent sample in OP and empty triangles represent samples during the 2nd World War (WW II).

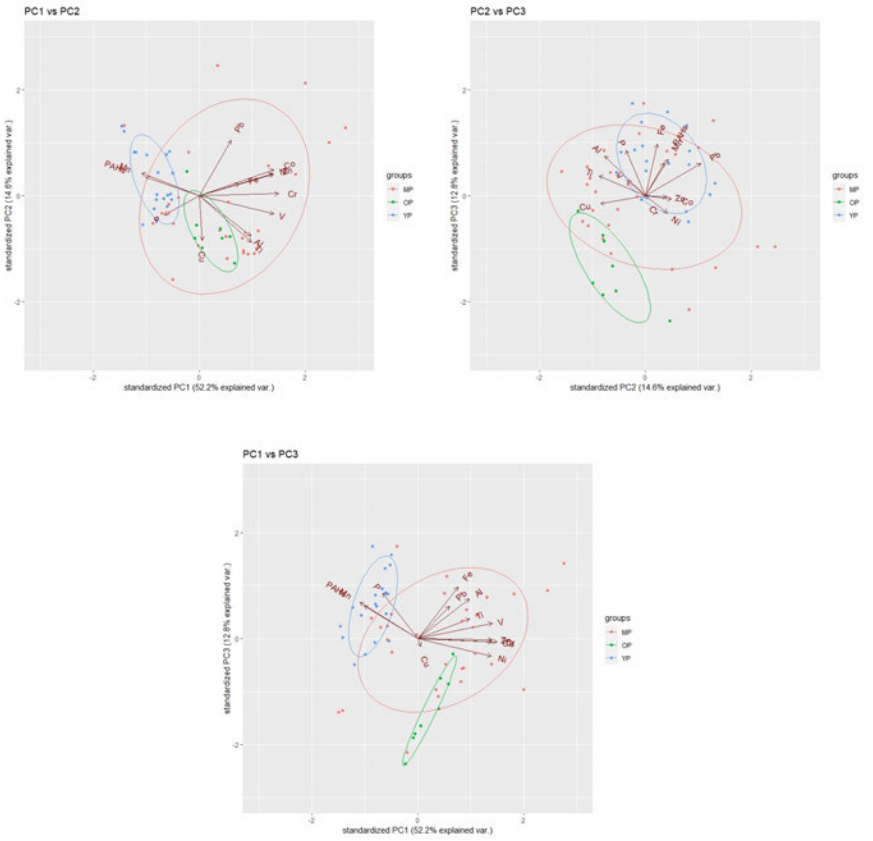

Fig. 5 C2 core PCA: the different major principal components against each other are reported in each graph plot, comparing trace elements, heavy metals, phosphorus and ΣPAHs. The legend shows the scores according to specific hydrometric phase: phase OP in green, phase MP in red and phase YP in blue.

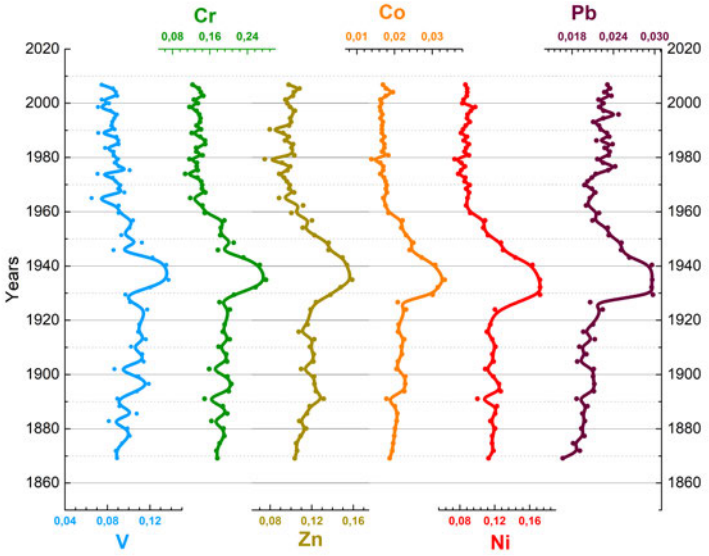

Fig. 6 Trace metal concentration (V, Cr, Zn, Co, Ni, Pb) temporal profiles of the C2 core (adjacent-averaging method, with weighted average options was used on 5 points to obtain the trends line)

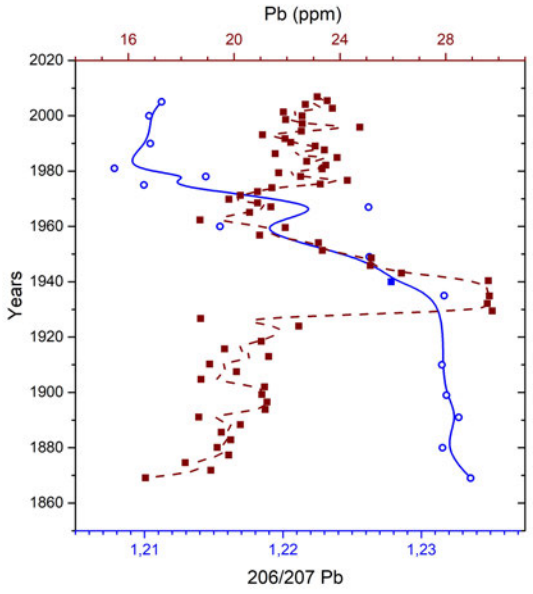

Fig. 7 Trends of total Pb concentration and $^{206}Pb/^{207}Pb$ isotope ratio, for the C2 core. The solid blue line indicates the 206/207 Pb isotope ratio, while the dashed brown line indicates the Pb concentration (ppm), and adjacent-averaging method, with weighted average options was used on 5 points to obtain the trends line.

Supplementary Files

This is a list of supplementary files associated with this preprint. Click to download.

- SMarticlePG1.pdf